TECHNISCHE MECHANIK, 30, 1-3, (2010), 195 – 202
submitted: October 31, 2009

On the thermomechanical-chemically coupled behavior of acrylic bone cements: Experimental characterization of material behavior and modeling approach

S. Kolmeder, A. Lion

This study presents a constitutive model that is able to describe the curing phenomena of acrylic bone cements used in vertebroplasty. During the surgery the initial liquid bone cement is injected into a porous vertebra and penetrates it depending on the applied pressure. The procedure is accompanied by an exothermal phase transition from a viscous fluid to a viscoelastic solid. Moreover chemical shrinkage, thermal expansion as well as changes in temperature can be observed. After curing the bone cement stabilizes the filled vertebra within the vertebral column according to Baroud et al. (2004a). To represent this thermomechanical-chemically coupled material behavior a physically-based theory of finite viscoelasticity is developed. A multiplicative decomposition of the deformation gradient into a mechanical, thermal and chemical part, as proposed by Lion and Höfer (2007), forms the basis of the constitutive model. The exothermal polymerization of the bone cement is specified by an additive contribution to the free energy depending on the degree of cure. Thereby a differential equation represents the process-dependent behavior of the degree of cure.
Experimental data supports the physical properties of the theory and provide information to parameterize the model. In detail, the time- and temperature-dependent exothermal curing behavior is studied with differential scanning calorimetry and with temperature-controlled rheometry. The structure of the constitutive model used to describe the material behavior of bone cement is motivated considering the experimental results.

1 Introduction

Polymethylmethacrylate (PMMA, also known as plexiglas) was clinically first used in the dental sector, after Otto Röhm invented the polymerisation of methacrylates in the late 1920s. Since 1960 bone cements on the basis of Polymethylmethacrylate have also been successfully established in joint arthroplasty surgery (DiMaio and Frank, 2002). Thereby the cement acts like a glue between the prosthesis and the bone and transfers loads from the prosthesis to the bone and vice versa. A relatively new field of application for bone cements is the treatment of collapsed vertebrae affected by osteoporosis. The so-called vertebroplasty is an operation technique where liquid bone cement is injected by means of a syringe through a biopsy needle into the porous vertebra. Once having filled the cavities caused by osteoporosis, the bone cement changes its phase from a viscous fluid into a viscoelastic solid. This phase transition is controlled by an autocatalytic exothermal curing reaction and is accompanied by shrinkage in volume. As a result the cured cement stabilizes the filled vertebra within the spinal column. However, several difficulties arise for the surgeon during the operation process. In order to achieve a successful surgery, on the one hand the cement should optimal penetrate the vertebra. Therefore, a high injection pressure and an injection at low viscosity are desirable. On the other hand the cement should not contact the surrounding tissue as high curing temperatures as well as leaking toxic monomer Methylmethacrylate (MMA) can cause necrosis, numbness and paralysis. Low injection pressure or high cement viscosity can help to prevent these complications. Moreover, the position of the hollow needle has great influence on the distribution of the viscous cement within the porous vertebra. Although X-ray observation of the radio-opacified cement supports the surgeon in the operation process there are still great difficulties in handling all degrees of freedom and circumstances.
A numerical simulation prior to the surgery process based on the finite element method can give information on the right choice of the parameters for a successful surgery and thus minimize the above mentioned risks. Several approaches have been made to model the material properties of bone cement partly or in a very simple manner (Mazzullo et al., 2002; Srimongkol et al., 2005; Baroud et al., 2004a,b). This study presents the mathematical modelling and experimental characterization of the time dependent curing behavior as well as the accompanied chemical shrinkage of acrylic bone cement. The mathematical description of the time dependent curing behavior forms the basis for a complex thermomechanical-chemically coupled material model, as for example introduced

by Lion and Höfer (2007), that accounts for the change in mechanical properties (e.g. complex shear modulus, coefficient of thermal expansion and chemical shrinkage) and thermomechanical properties (e.g. heat capacity, thermal conductivity and heat release) with proceeding polymerisation. Implemented in a finite element program, the developed material model should be capable to describe the flow of the bone cement from the syringe through the biopsy needle and reflect the dispersion of the cement within the cavities of the vertebra. It should also give precise information on the local temperature distribution and change in volume.

2 Bone cement material

2.1 Composition

Acrylic bone cements are mixed of two components: a polymer in powder form and a liquid monomer. The polymer powder consists of spherical PMMA or MMA copolymers in the range of 50 μm and contains the initiator dibenzoyl peroxide (BPO), the radio pacifier, usually zirconium dioxide or barium sulphate, for visibility under X-ray observation, antibiotics and a dye for coloring. The latter three ingredients do not take part in the curing process (Kühn et al., 2005). The differences in the composition of the polymer significantly influence the physical properties of the cement. MMA is the main ingredient of the liquid monomer and includes dimethyl-para-toluidine (DMpT) as an activator and also a dye. Small amounts of hydroquinone are added to avoid polymerisation of the liquid while stored.

2.2 Radical polymerisation

Two different processes start when the polymer powder and the monomer liquid are mixed together. A physical dissolution of the monomer and polymer produces a viscous fluid, often referred to as a dough (Kühn et al., 2005), and a chemical polymerisation that causes the final hardening of the bone cement. For the initial chemical reaction the initiator BPO and the activator DMpT create free radicals which trigger the polymerisation of MMA. The number of generated free radicals determines the speed of polymer chain growth and hence, the conversion of MMA to PMMA. Chain growth is terminated if two reactive chain ends meet and build a non reactive polymer molecule. The heat generation during the exothermal polymerisation is 57 kJ per mole MMA (molar mass of MMA is 100 g) and is responsible for temperature peaks. The radiopacifier and the powder to liquid ratio influence this specific heat generation.
As the number of molecules changes during polymerisation, the density of the cement increases. Pure MMA shows a shrinkage in volume of 21 %. Depending on the powder to liquid ratio commercial bone cements have a volume shrinkage of approximately 7 % (Kühn et al., 2005).

3 Mathematical model

Several phenomenological based models exist to mathematically describe the kinetics of exothermal curing reactions (Akkerman et al. (1998); Kim and Char (1999); Simon et al. (2000) among many others). Because curing reactions show autocatalytic behavior, i.e. the reaction speed increases with an increasing degree of cure and decreases as solidification inhibits diffusion, these models have a rate-dependent form. To quantify the progress of the chemical reaction we define the degree of cure q, also referred to as chemical coordinate, as follows:

$$q(t) = \frac{H(t)}{H_u} \qquad \text{with} \qquad H(t) = \int_0^t \left(\frac{dQ}{d\bar{t}} \right) d\bar{t} \tag{1}$$

whereas $\frac{dQ}{dt}$ is the rate of released heat of reaction at the current reaction time t and H_u is the ultimate heat of reaction after all educts have been converted completely. The evolution equation we use is based on an autocatalytic model, proposed by Sourour and Kamal (1976) and has the form:

$$\frac{dq}{dt} = (K_1 + K_2 \cdot q^{\alpha})(1-q)^{\beta} \tag{2}$$

α and β are interdependent material parameters (e.g. $\alpha + \beta = 3$) that have to be identified and generally do not change with temperature.

K_1 and K_2 are thermally activating parameters and can be specified by an Arrhenius-equation:

$$K_i = K_{i0} \exp\left(\frac{-E_i}{RT}\right) \qquad i = 1, 2 \tag{3}$$

K_{10}, K_{20}, E_1 and E_2 are material parameters to be determined and $R = 8.314\, J/molK$ is the universal gas constant. However, the above equations do not take into account that the polymerisation is decelerated as a result of vitrification effects, if the glass temperature rises above curing temperature. The reaction is then no longer concentration controlled but diffusion-controlled. This effect is due to the dependence of the glass temperature on the degree of cure, i.e. the glass temperature increases with an increasing cross linking. Unless the curing temperature lies above the glass temperature of the completely cured material the attainable degree of cure will always be smaller than 1 (Wenzel, 2005). Fournier et al. (1996) therefore expand equation 2 by an empirical diffusion factor.

$$\frac{dq}{dt} = (K_1 + K_2 \cdot q^{\alpha})(1-q)^{\beta} f_D(q) \qquad \text{with} \qquad f_D(q) = \left[\frac{2}{(1 + \exp[(q - q_{end})/b]} - 1\right] \tag{4}$$

whereas b is an empirical material specific constant and q_{end} is the maximum attainable degree of cure and depends on the curing temperature. In order to calculate the maximum attainable degree of cure at a certain reaction temperature usually the DiBenedetto equation is evaluated (Blumenstock, 2003; Wenzel, 2005).

$$\frac{T_g(q) - T_{g,0}}{T_{g,1} - T_{g,0}} = \frac{\lambda q}{1 - (1-\lambda)q} \tag{5}$$

However, in the case of bone cement a linear approach of the following kind seems to be more suitable:

$$\frac{T_g(q) - T_{g,0}}{T_{g,1} - T_{g,0}} = \lambda q + \gamma \tag{6}$$

In equation 5 and 6 $T_g(q)$ is the glass transition temperature at the degree of cure q, $T_{g,0}$ the glass transition temperature at the degree of cure 0 and $T_{g,1}$ the glass transition temperature at the degree of cure 1. The material parameters λ and γ have to be fitted to measured data. By rearranging equation 6 we get:

$$q_{end} = \frac{f(T) - \gamma}{\lambda} \qquad \text{with} \qquad f(T) = \frac{T_{iso} + \Delta T - T_{g,0}}{T_{g,1} - T_{g,0}} \qquad \text{and} \qquad T_g(q_{end}) = T_{iso} + \Delta T \tag{7}$$

For isothermal reaction temperatures lower than the maximum glass temperature $T_{g,1}$ a glass temperature is reached which is approximately $\Delta T = 20\, K$ above curing temperature. The reaction comes to a stop because of diffusion control (Wenzel, 2005).

4 Measurements

A commercial bone cement was used for all measurements

4.1 Calorimetric Measurements

In order to identify the paramters K_{10}, K_{20}, E_1, E_2 in equation 3, α, b in equation 4 and λ in equation 5, isothermal curing experiments were carried out with a differential scanning calorimeter DSC 204 F1 Phoenix, manufactured by Netzsch. For these tests samples of mixed bone cement of weight ranging from 5 to 8 mg were encapsulated in pierced standard aluminum pans. The powder and liquid component were prechilled in a refrigerator at a temperature of $5\,^{\circ}C$ and took out directly before mixing to ensure the degree of cure is very close to zero when starting the measurements. Moreover, the samples were placed in the differential scanning calorimeter (DSC)

oven at 220 ± 10 seconds after the two components were merged together. A very small loss in weight could be detected by measuring the samples before and after the experiments, but it can be neglected for further calculations. Measurements were done from 15 to $65\,°C$ at steps of $5\,°C$ as this is the range of interest for the surgery process of vertebroplasty. During the experiment the oven temperature was kept constant for one hour and the heat flow dQ/dt was measured. Afterwards, the sample was cooled down by $20\,°C$, heated up to $150\,°C$ and cooled down to $20\,°C$ three times at a heating rate of $10\,°C/min$. The isothermal phase provides the data to determine the heat release and rate of cure at a certain curing temperature. The following temperature ramp yields the remaining heat of reaction to reach a degree of cure of 1 due to post-curing. The DSC signal, i.e. the heat flow dQ/dt, should be identical for the second and third ramp since the exothermal reaction is completely finished (see figure 4). Figure 1 shows the DSC-signals of the isothermal curing phases at different temperatures for a duration of one hour.

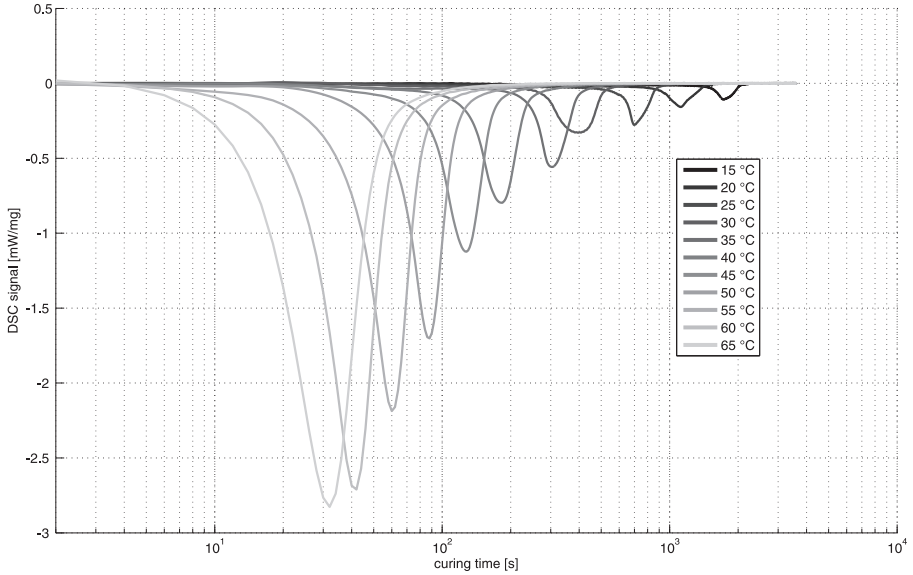

Figure 1: DSC-signals of curing bone cement at different isothermal curing temperatures

4.2 Shrinkage Measurements

The shrinkage measurements are performed using Archimedes principle. A balance of type ME235P from Sartorius (resolution $0.01\,mg$) is mounted over a Lauda cooling thermostat RE207 as shown in figure 2. The thermostat is filled with 5 litres of silicone oil which can be tempered from $-40\,°C$ up to $200\,°C$. Specimens of fluid bone cement with a typical weight of $4\,g$ are sealed between two thin walled foils out of Polyethylene. The weight of the foils is about $0.015\,g$ and hence can be neglected. To ensure an effective heat convection and thus a constant curing temperature the specimens have the form of flat discs measuring approximately $35\,mm$ in diameter and $1-3\,mm$ in height. After weighing the sealed specimen it is spiked by a fishing-hook attached to a thin nylon thread. The other end of the nylon thread is directed through a hole in the frame and fixed to a hook on the bottom of the scale (see figure 2). Subsequently the specimen is dipped into the preconditioned silicone oil and the weight is recorded continuously. An additional PTC-resistor connected to a Labjack measurement device via a Wheatstone bridge detects the temperature adjacent to the specimen. All devices are connected to a computer and the data is evaluated online in the following manner:

$$F_{buoyancy} = \rho_{fl}(T) V_{sp} g \tag{8}$$

whereas $F_{buoyancy}$ is the buoyancy force of the dipped specimen, $\rho_{fl}(T)$ is the temperature dependent density of the silicone oil, V_{sp} is the volume of the specimen and g is the acceleration of gravity. By rearranging equation 8, we get:

$$\rho_{sp} = \rho_{fl}(T)\frac{m_{sp}}{m_{sp} - F_{g,fl}/g} \qquad \text{with} \qquad F_{buoyancy} = m_{sp}g - F_{g,fl} \qquad \text{and} \qquad V_{sp} = \frac{m_{sp}}{\rho_{sp}} \tag{9}$$

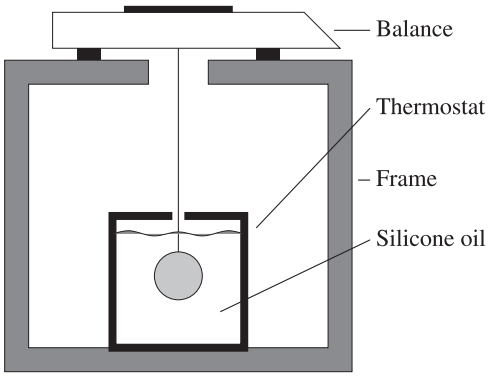

Figure 2: Measurement setup for shrinkage experiment

Thus the density of the specimen ρ_{sp} can be calculated by knowing the density of the silicone oil ρ_{fl}, the specimen's mass m_{sp} and the weight of the dipped specimen $F_{g,fl}/g$.
Isothermal shrinkage measurements were done from 15 to 50 $°C$ also at steps of 5 $°C$. The procedure for mixing the cement was identical to the one for the DSC experiments. The time from starting the mixing until dipping the specimens into the silicone oil was also around 220 seconds. The results can be seen in figure 3. At the very beginning of the experiments a thermal expansion or contraction of the uncured specimens can be observed due to the temperature difference between the specimens and the silicone oil.

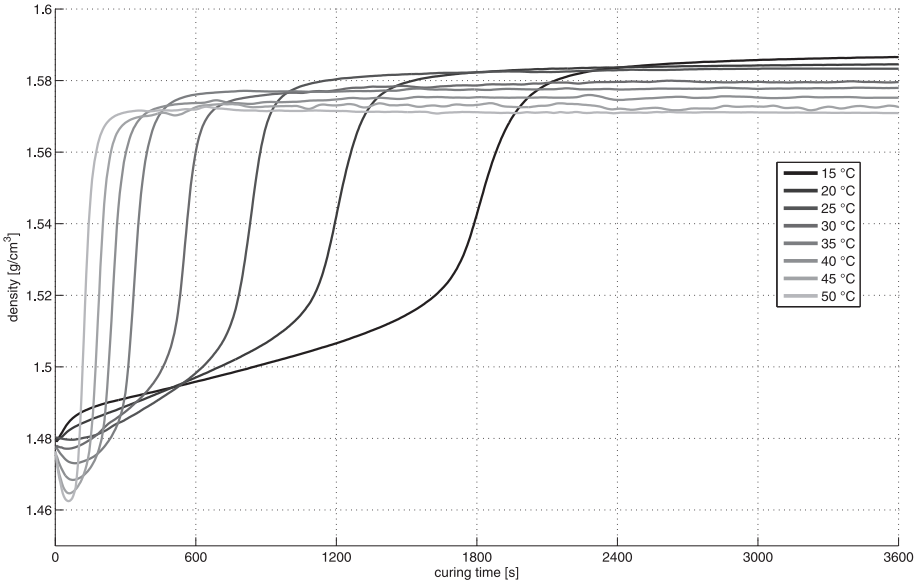

Figure 3: Density of curing bone cement at different isothermal curing temperatures

5 Analysis and Results

5.1 Reaction Kinetics

The ultimate heat of reaction according to the temperature program described in section 4.1 is composed of the heat release during the isothermal phase and the first heating ramp. By integrating the course of $\frac{dQ}{dt}$ for the isothermal phase, i.e. the curves in figure 1, the first fraction of the ultimate heat can be calculated. However, for the temperature ramp a baseline has to be determined. Assuming the specific heat capacity is only a function of temperature (and not of degree of cure) for the solidified material, the second or third heating ramp can serve as a baseline with an adjusted time scale (see figure 4). The overshooting at the very beginning of figure 4 is generated by the change of an isothermal phase into a temperature ramp. The released heat of post-curing can thus be

identified as area between the curves of the first and second or third heating ramp, respectively (see figure 4). With this data the degree of cure can be computed for every time step during the isothermal curing phase. Moreover, the glass temperature of the completely cured state $T_{g,1}$ has been measured as $105\,°C$ and for the uncured state as $-50\,°C$.
For the parameters λ and γ in equation 6 the following values were obtained:

$$\lambda = 2.5021 \quad \gamma = -1.3592$$

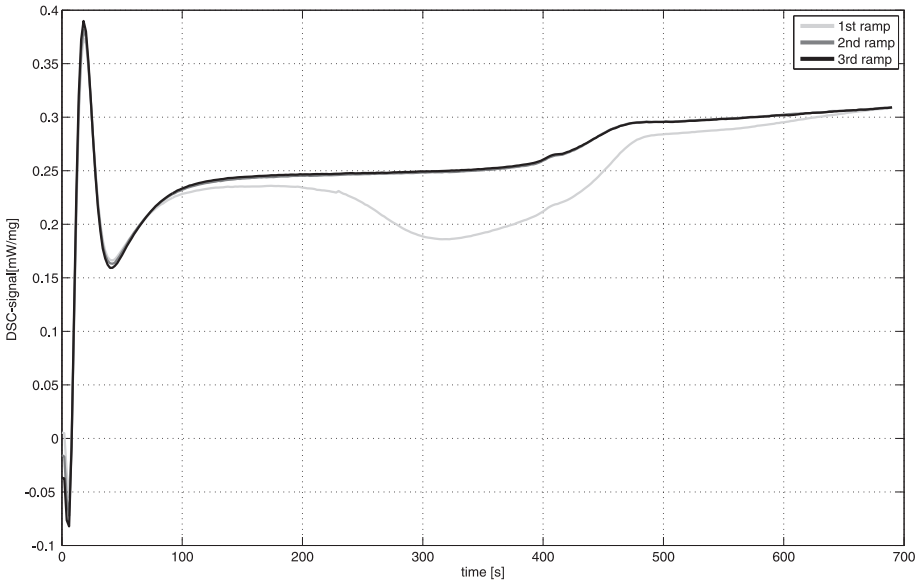

Figure 4: DSC-signal for 1^{st}, 2^{nd} and 3^{rd} temperature ramp

In order to determine the parameters of equations 3 and 4 the following procedure was applied. First, the data for the degree of cure and for the rate of cure were scaled to their corresponding degree of cure. The values for K_1, K_2, α (β was chosen as 3) and b were identified with a non linear least-square method for each temperature separately. Next, the values were used to fit equation 3 to get starting values for K_{10}, K_{20}, E_1 and E_2. At last this data was the starting point for the final parameter identification also applying a non linear least-square algorithm. The resulting values were:

$$\begin{array}{ll} K_{10} = 1.792 \cdot 10^{10} & E_1 = 7.964 \cdot 10^4\, J/mol \\ K_{20} = 3.234 \cdot 10^6 & E_2 = 4.571 \cdot 10^4\, J/mol \\ \alpha = 2.050 & b = 1.917 \end{array}$$

A comparison between model and experiments can be seen in figure 5, whereas the solid lines represent the experimental data and the dashed lines represent the model data.

5.2 Shrinkage

Figure 3 and 5 propose that the degree of cure and the shrinkage in volume are directly related to each other. To check a correlation the relative shrinkage in volume based on the minimal values of the density in figure 3 was calculated. Furthermore, the mathematical model (equation 4) was evaluated at the time steps of the shrinkage measurement and the relative shrinkage in volume was plotted versus the associated degree of cure (see figure 6).

A good correlation between the degree of cure and the volume shrinkage can be observed in figure 6. Deviations from a direct proportionality between the degree of cure and the shrinkage in volume may be caused by differences of the reaction kinetics from the measurements, heating or cooling of the specimens after the dipping into silicone oil and the choice of the basis for the calculation of the relative shrinkage in volume.

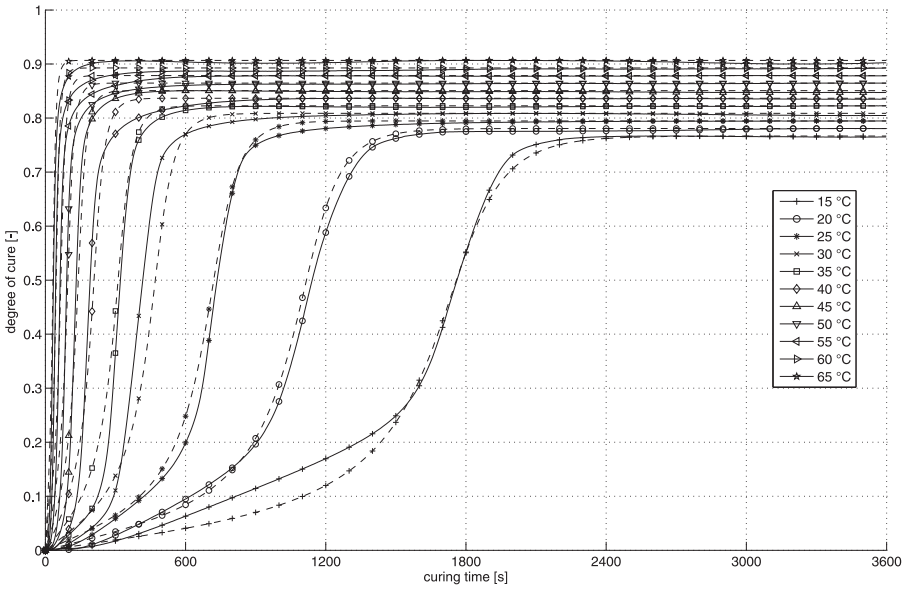

Figure 5: Comparison between model data (dashed lines) and experimental data (solid lines) for the degree of cure

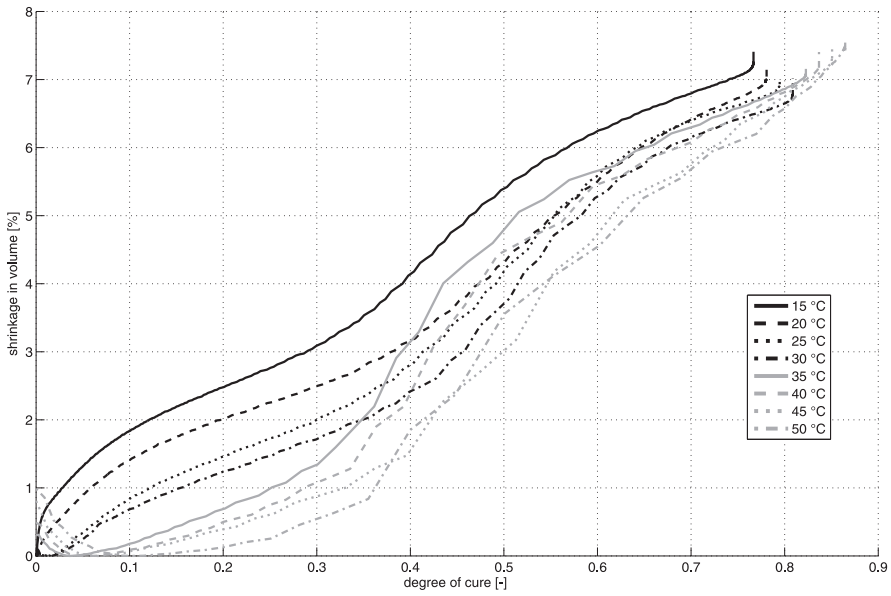

Figure 6: Shrinkage in volume versus degree of cure

6 Summary

An applicable model for the prediction of the curing phenomena of acrylic bone cements over a wide temperature range is presented. The model takes into account the incomplete curing at curing temperatures lower than the final glass transition temperature. With means of experimental data the parameters of the model are identified for a commercial bone cement. In addition the shrinkage behavior during the isothermal cure process is examined. The correlation between the shrinkage in volume and the degree of cure support the theoretical assumption of a direct proportionality.

References

Akkerman, R.; Wiersma, H.; Peeters, L.: Spring-forward in continuous fibre-reinforced thermosets. In: J. Huetink; F. Baaijens, eds., *Simulation of Materials Processing: Theory, Methods and Applications: Numiform98*, pages 471 – 476, Balkema, Rotterdam (1998).

Baroud, G.; Bohner, M.; Heini, P. F.; Steffen, T.: Injection of biomechanics of bone cements used in vertebroplasty. *Bio-Medical Materials and Engineering*, 14, (2004a), 487 – 504.

Baroud, G.; Vant, C.; Giannitsios, D.; Bohner, M.; Steffen, T.: Effect of vertebral shell on injection pressure and intravertebral pressure in vertebroplasty. *Spine*, 30, (2004b), 68 – 74.

Blumenstock, T.: *Analyse der Eigenspannungen während der Aushärtung von Epoxidharzmassen*. Ph.D. thesis, Universität Stuttgart (2003).

DiMaio, D.; Frank, R.: The science of bone cement: A historical review. *Orthopedics*, 25, (2002), 1399 – 1407.

Fournier, J.; Williams, G.; Duch, C.; A., A. G.: Changes in molecular dynamics during bulk polymerization of an epoxide-amine system as studied by dielectric relaxation spectroscopy. *Macromolecules*, 29, (1996), 7079 – 7107.

Kim, H.; Char, K.: Dielectric changes during the curing of epoxy resin based on diglycidyl ether of bisphenol a (dgeba) with diamine. *Bulletin of the Korean Chemical Society*, 20, (1999), 1329 – 1334.

Kühn, K.-D.; Ege, W.; Gopp, U.: Acrylic bone cements: composition and properties. *Orthopedic Clinics of North America*, 36, (2005), 17 – 28.

Lion, A.; Höfer, P.: On the phenomenological representation of curing phenomena in continuum mechanics. *Archives of Mechanics*, 59, (2007), 59 – 89.

Mazzullo, S.; Paolini, M.; Verdi, C.: Numerical simulation of thermal bone necrosis during cementation of femoral prostheses. *Journal of Mathematical Biology*, 29, (2002), 475 – 494.

Simon, S.; McKenna, G.; Sindt, O.: Modelling the evolution of the dynamic mechanical properties of a commercial epoxy during cure after gelation. *Journal of Applied Polymer Science*, 76, (2000), 495 – 508.

Sourour, S.; Kamal, M.: Differential scanning calorimetry of epoxy-amine cure: isothermal cure kinetics. *Thermochimica. Acta*, 14, (1976), 41 – 59.

Srimongkol, S.; Wiwatanapataphee, B.; Wu, Y.: Computer simulation of polymethylacrylate bone cement flow through femoral canal and cancellous bone. *Anziam J. (EMAC2005)*, 47, (2005), C404 – C418.

Wenzel, M.: *Spannungsbildung und Relaxationsverhalten bei der Aushärtung von Epoxidharzen*. Ph.D. thesis, Technische Universität Darmstadt (2005).

Address: Dipl.-Ing. (FH) Sebastian Kolmeder and Univ.-Prof. Dr.-Ing. habil. Alexander Lion, Institut für Mechanik (Luft- und Raumfahrttechnik), Universität der Bundeswehr München, D-85579 Neubiberg.
email: `sebastian.kolmeder@unibw.de; alexander.lion@unibw.de.`